

# Academic Journal of Chemistry

ISSN(e): 2519-7045, ISSN(p): 2521-0211

Vol. 2, No. 12, pp: 134-142, 2017

URL: <http://arpgweb.com/?ic=journal&journal=20&info=aims>

## Photocatalysis of Chlorazole Black E Dyes Using Titanium Dioxide Doped With Iron (Fe-TiO<sub>2</sub>)

Amana B. S.\*

Nigerian Institute of Leather and Science Technology, Samaru-Zaria, Nigeria

Yilleng M.

Department of Chemistry, Kaduna State University, Agwan Rimi Kaduna, Nigeria

Ayebe B.

Nigerian Institute of Leather and Science Technology, Samaru-Zaria, Nigeria

Tanko S. F.

Nigerian Institute of Leather and Science Technology, Samaru-Zaria, Nigeria

putshaka J. D.

NILEST Extension Centre, Abbaotir Jos Plateau State

Akabuogu E. P.

Nigerian Institute of Leather and Science Technology, Samaru-Zaria, Nigeria

**Abstract:** Fe-TiO<sub>2</sub> catalyst was implemented for photo mineralization of chlorazole black E dye. Percentage conversion. 67.2% , 74.8% and 62.8% using 1%, 3% and 5% Fe-TiO<sub>2</sub> under Visible light and 73.3%, 67.2% and 62.8% using 1%, 3% and 5% Fe-TiO<sub>2</sub> under UV light after irradiation for 80 Minutes respectively. Fe-TiO<sub>2</sub> under UV/Visible light has proven to be effective through the investigation which was synthesized through wet-impregnation, calcined and characterized to determine the group resulting from bond vibrations using FT-IR and crystalline phase of the catalyst via XRD pattern. It was then subjected to photo-degradation to optimize various experimental parameters such as effects of metal loads, light source and time. The obtained results are shown in decreasing order of activity 3% Fe-TiO<sub>2</sub> > 1%Fe-TiO<sub>2</sub> >5%Fe-TiO<sub>2</sub>. Which indicate that 3% Fe-TiO<sub>2</sub> shows more photo-degradation at UV/Visible but does more better at visible region with respect to time.

**Keywords:** Photodegradation; Black E dyes; Fe-TiO<sub>2</sub> catalyst.

### 1. Introduction

Dyes are widely used in the textile, paper, plastics, leather, food and cosmetics industries to colour their products. Effluents from these industries put a huge burden to the environment when discharged indiscriminately, [1]. Acid azo dyes make up about a half of all known dye stuffs in the world, making them the largest group of synthetic colourants released into the environments [2]. Semiconductor photocatalysis is a technique with great potential to control aqueous organic contaminants or air pollutants, It holds several advantages over conventional oxidation processes [3-7].

The nano-TiO<sub>2</sub> photocatalyst is a well-known photocatalyst among the metal oxides recognized for its high efficiency, low cost, physical and chemical stability, widespread availability, and noncorrosive property [8, 9]. Many recent studies have been reported on the photodegradation of the organic compounds in industrial waste water in the presence of TiO<sub>2</sub> photocatalysts using iron as a dopant metal to overcome the limitations of nano-TiO<sub>2</sub> [10-13], in attempt to improve the photocatalytic activity of TiO<sub>2</sub> in the visible region, such as a wide band gap, ineffectiveness of photocatalysis under sunlight, and thermal instability [11].

However, many efforts have been made to achieve the utilization of visible light for TiO<sub>2</sub> material, such as transitional metal ion doping [10]. Basically, nano-TiO<sub>2</sub> can only utilize 6% of the total solar irradiation in photocatalysis due to the large band gap of anatase.

Among the results reported in literature for iron doped photocatalysts used for wastewater treatment for the degradation of various organic pollutants including photodegradation of Active Yellow XRG [14, 15], phenol [16], Malachite Green (MG) [17] benzoic acid [18], 4-Nitrophenol [18, 19], Nitrite and nitrate ions [20] under UV and visible light irradiation.

Various technologies are available for the treatment of dye contaminated wastewater such as, adsorption, electrochemical [21, 22].

Adsorption, [23], biodegradation via free and immobilized cells, [24], photocatalytic degradation, [25] electrochemical oxidation, [22, 26], and ionexchange [27] Most physico-chemical methods are expensive and are greatly affected by other wastewater constituents, or generate waste products that need to be handled. Also, azo dyes

can withstand conventional aerobic wastewater treatment processes and their persistence is mainly due to the presence of sulfo and azo groups that do not occur naturally [28].

Adsorption is considered as one of the best treatment technologies among all of the above as it is a simple, fast and efficient process, which does not generate any hazardous by-products. The use of natural adsorbents has been widely studied for dye removal, yet they are also associated with separation issues. Averrhoa carambola extract (ACE) was exploited as a novel and green stabilizer in the synthesis of stabilized magnetite nanoparticles (SMNPs), which were used for the removal of chlorazole black E from wastewater [29, 30].

Utilization of a zeolite-Y supported  $\text{TiO}_2$  catalyst for the photocatalytic demineralization and full kinetic characterization of Chlorazole Black E (Direct Black 38) dye was reported [9]. Dye concentration, pH of dye solution, conductivity and temperature during photodegradation were utilized in this study [9].

This paper appraises a different doping technique [31] that widens the photocatalytic range from the ultraviolet to the visible light region, thus allowing for the photocatalytic degradation of organic pollutants under solar irradiation.

## 2. Materials and Methods

### 2.1. Catalyst Preparation

The titanium dioxide support was prepared according to method described earlier [7], 14.68g and 0.32g of ferrous Nitrate was dissolved in 100ml distilled water as per wet-impregnation method. The solution was then placed on the mechanical stirrer of high revolution for wet-impregnation of ferrous nitrate precursor at ambient temperature, under vigorous mixing for 1hr. after which the obtained ferrous nitrate impregnated titanium dioxide mass was then oven dried at  $150^\circ\text{C}$  for 24hrs. The dried solid mass was then finally subjected to calcinations using muffle furnace at  $600^\circ\text{C}$  for 2hrs, to develop the Fe- $\text{TiO}_2$ .

Identical procedure was applied for making catalyst with different ferrous nitrate to titanium dioxide weight ratio in order to analyse the effects of ferrous nitrate loading on the properties of the catalyst.

### 2.2. Photodegradation of Chlorazole Black E Dye

The photo degradation of chlorazole black E was carried out using UV-fluorescence cabinet analysis with different AOPS such as UV/ $\text{Fe-TiO}_2$  and visible/ $\text{Fe-TiO}_2$  to identify the most suitable and economical process for complete decolourization and substantial mineralization of the dye. The effect of various experimental parameters such as time of irradiation, metal loading and light source was carried out to arrive at optimized experimental condition. The dye stock solution (100ml) of  $1 \times 10^{-5}$  g/l concentration and 1g of  $\text{Fe-TiO}_2$  were prepared. The experiments were carried out in batch-type photo reactor.  $\text{Fe-TiO}_2$  acts as the catalyst and UV light as illuminating light source. The dye solution were stirred and 10ml samples are withdrawn using syringe at regular time interval of 20 minutes and centrifuged, the dye concentration were measured spectrophotometrically and the same procedure was carried out using visible light to study the decolourisation and degradation.

Fig-1. Chlorazole black E (Direct Black 38) Dye Molecular Structure.

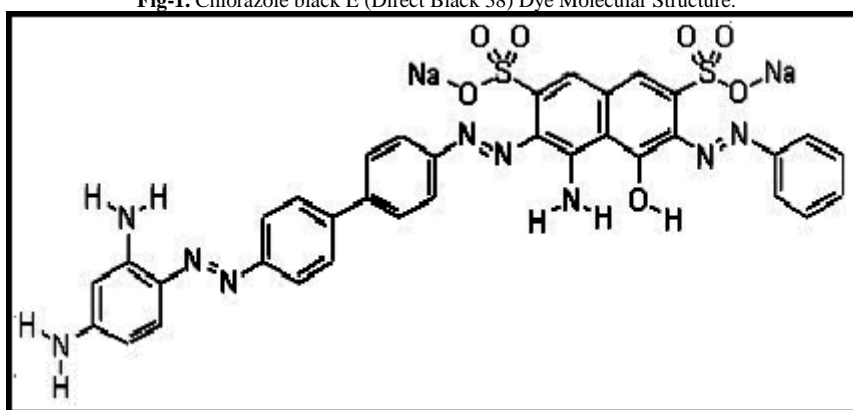


Plate-1. Photo reactor (UV/Visible Florescent Analysis cabinet)



### 3. Results and Discussion

#### 3.1. XRD

Figure 2 shows the XRD pattern of 1%Fe-TiO<sub>2</sub>. From the XRD pattern it was observed that there were three major peaks found at 24.9811, 27.0112, and 33.6206°. The strongest peak at 27.0112° with corresponding intensity ratio of 100 is assigned to the Fe used in modifying the titanium dioxide which exists as hematite when compared with the PDF Card no 33-0664. The 2<sup>nd</sup> prominent peak subtends at 2Theta Bragg's angle 24.9811 with corresponding intensity ratio 59 is assigned to the anatase phase of titanium dioxide present in the support when compared with the PDF file number 21-1272. The 3<sup>rd</sup> strongest peak subtends at 2Theta Bragg's angle 33.6206 with corresponding intensity ratio 42 is attributed to the rutile phase of titanium dioxide when compared with the PDF file number 21-1276. Close observation on the individual strongest peaks, have some residual peaks (minor peaks). These are found at the 2Theta angle corresponding to angles 30.8289, 45.1507 and 60.2342 respectively.

However, the major minerals content in sample-Iron 1% as confirmed by the various peaks against corresponding 2Theta Bragg's angle are: Hematite, rutile and anatase.

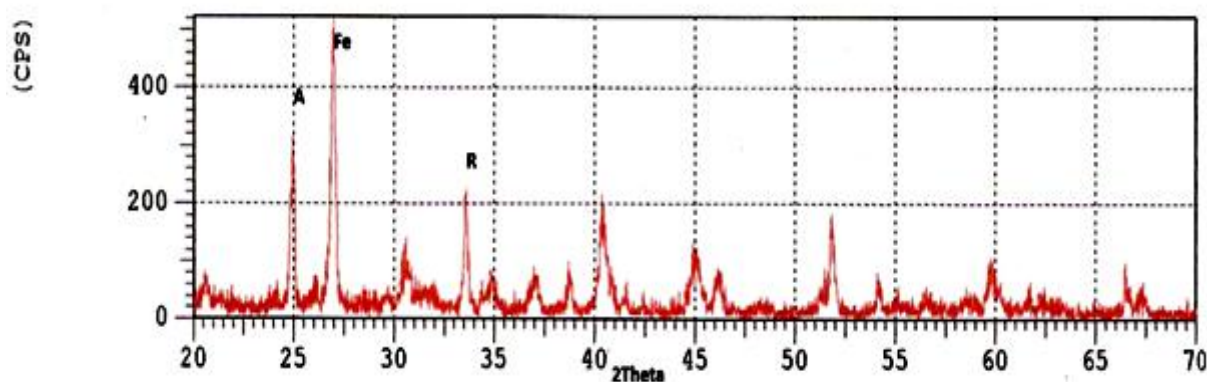
Fig-2. XRD Pattern of 1% Fe-TiO<sub>2</sub>

Figure 3, of the XRD pattern of 3% Fe-TiO<sub>2</sub>. From the XRD pattern it was observed that there were three major peaks found at 28.3669, 24.8670 and 38.5761°. The strongest peak at 28.3669 with corresponding intensity ratio 100 is attributed to Fe used in modifying the titanium dioxide which exist as hematite when compared with the card no 33-0664. The 2<sup>nd</sup> strongest peaks subtends at 2Theta Bragg's angle 24.8670° with corresponding intensity ratio 27 is assigned to anatase phase of the titanium dioxide present in the support when compared with the PDF file number 21-1272. the 3<sup>rd</sup> strongest peaks subtends at 2 Theta Bragg's angle 38.5761° with corresponding intensity ratio 27 is assigned to rutile phase of the titanium dioxide present in the support when compared with the PDF file number 21-1276. Close observation on individual strongest peaks have some residual peaks (minor peaks). These are found at the 2Theta Bragg's angles 42.3798 and 54.0281 respectively.

The major minerals contained in sample-Iron 3% as confirmed by the various peaks against corresponding 2Theta Bragg's angle are: Anatase, rutile and hematite, the minor minerals found are Eskolaite.

Fig-3. XRD Pattern of 3% Fe-TiO<sub>2</sub>

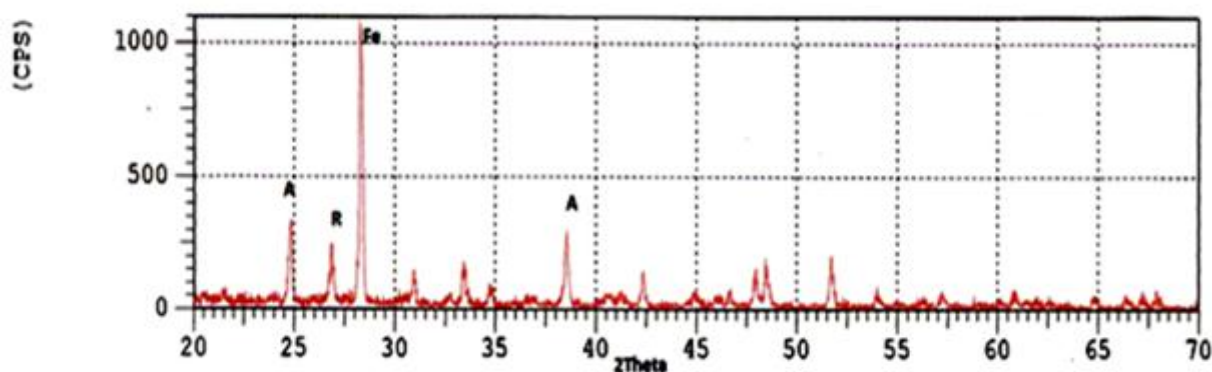
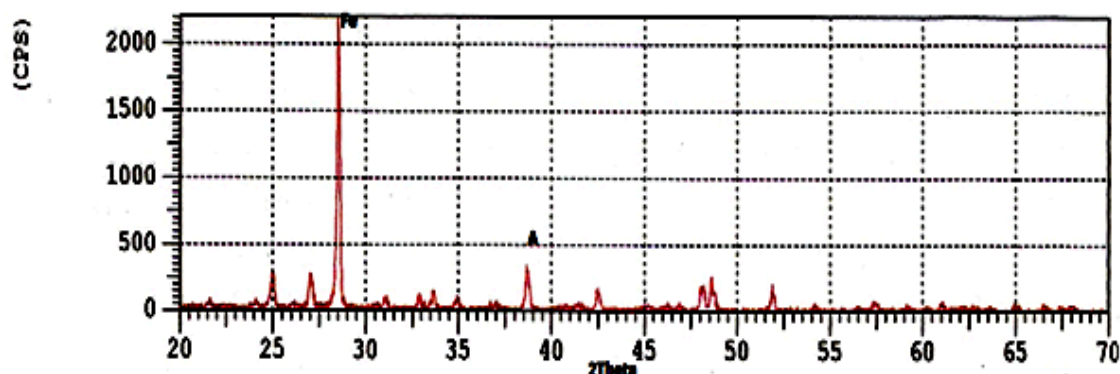


Figure 4 shows the XRD pattern of 5% Fe-TiO<sub>2</sub>. From the XRD pattern it was observed that there were three major peaks found at 28.5829, 38.7313 and 48.6571° the 1<sup>st</sup> strongest peak subtends at 2Theta Bragg's angle 28.5829 with corresponding intensity ratio 100 is assign to Fe used in modifying the titanium dioxide which exist as hematite when compared with the PDF file number 5-0561. The 2<sup>nd</sup> strongest peak at 38.7313 with corresponding intensity ratio 16 is attributed to anatase phase of titanium dioxide present in the support when compared with the PDF file number 21-1272.

The major minerals contained in sample-Iron 5% as confirmed by the various peaks against corresponding 2Theta Bragg's angle are hematite, anatase and maghamite.

Fig-4. XRD Pattern of 5% Fe-TiO<sub>2</sub>



### 3.2. FT-IR Spectra

Fourier Transform spectra (FT-IR) of 1, 3 and 5% Fe-TiO<sub>2</sub> after photodegradation of Chlorazole black E, were carried out using Shimadzu spectrophotometer, are shown in Figures (5-7).

FTIR spectrum of 1% Fe-TiO<sub>2</sub> is shown in Figure 5. Vibrations were observed at different frequencies. From 1422.55cm<sup>-1</sup> is assigned to C-O-H due to carboxylic derivative broken from chlorazole azo black E molecule. From this vibration 2523.94cm<sup>-1</sup> shows O-H due to the present of phenolic group in the dye molecule. The vibrations at 1793.86cm<sup>-1</sup>, 2977.23cm<sup>-1</sup> and 3463.30cm<sup>-1</sup> indicate C=O, CH<sub>3</sub>, CH<sub>2</sub> and N-H were due to carboxylic, methyl, methine and primary amine form as intermediate in the process of photodegradation.

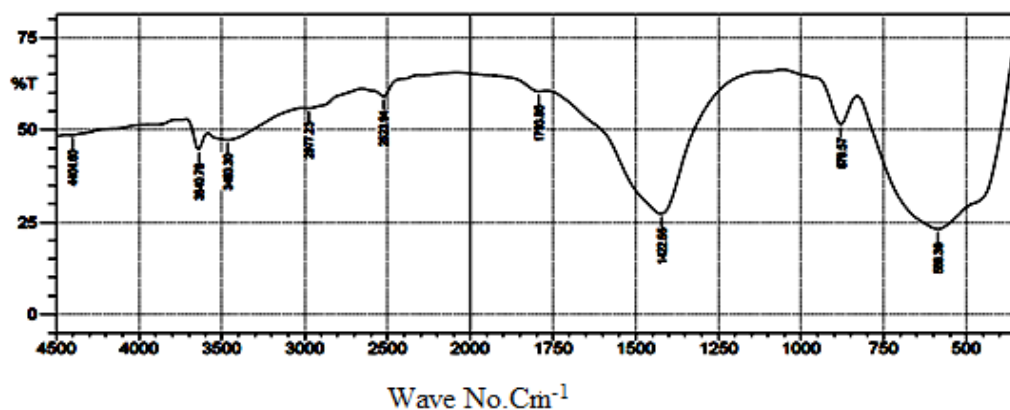
Fig-5. FTIR spectrum of used 1% Fe-TiO<sub>2</sub> after Photodegradation of Chlorazole black E.

Figure 6 Shows FTIR spectrum of 3% Fe-TiO<sub>2</sub> above, two vibrations at the following frequencies 1432.19cm<sup>-1</sup> and 3461.31cm<sup>-1</sup> were attributed to C-O-H, and N-H, indicate the presence of carboxylic derivative and primary amine broken down from the dye molecule during mineralization of chlorazole azo black E,

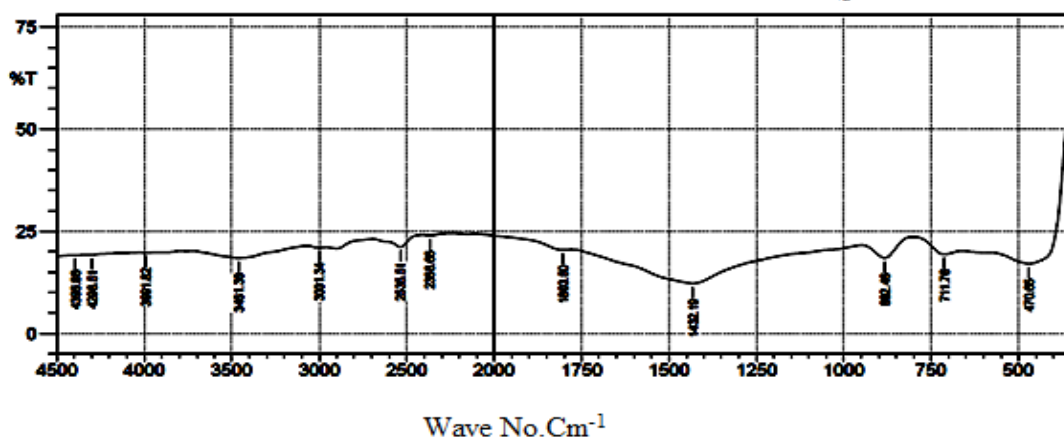
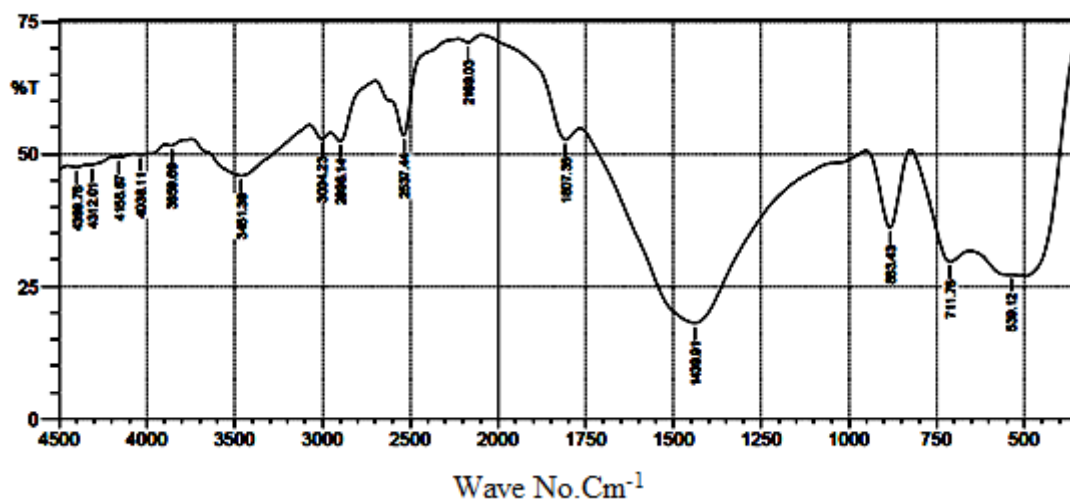
Fig-6. FTIR spectrum of used 3% Fe-TiO<sub>2</sub> after photodegradation of chlorazole black E.

Figure 7 shows FTIR spectrum of 5% Fe-TiO<sub>2</sub>, at different frequencies. The vibration at 1439.91cm<sup>-1</sup> is attributed to C-O-H due to carboxylic derivative, also vibration at 2537.44cm<sup>-1</sup> is assign to O-H which shows the presence of phenolic stretch. At vibration at 3004.23cm<sup>-1</sup> and 2898.14cm<sup>-1</sup> indicate C-H and CH alkanes form as a result of bond cleavage, however at 3461.38 cm<sup>-1</sup> is attributed to N-H which are primary amine obtained from photocatalytic degradation of chlorazole azo black E using UV and visible light.

Fig-7. FTIR spectrum of used 5% Fe-TiO<sub>2</sub> after photodegradation of chlorazole black E.

### 3.4. Effect of Time in Photo Degradation of Chlorazole Black E Dye Under UV and Visible Light are Shown as Figures (8-11).

#### 3.4.1. Effect of Time in Photo degradation of Chlorazole Black E dye

In this experiment, 0.2g of the catalyst was taken into 100ml  $1.0 \times 10^{-5}$  molar aqueous solution of chlorazole black E. The percentage photocatalytic degradation of chlorazole black E against time is shown in Figures 9 and 11, there observed the percentage conversion was 67.2%, 74.8% and 62.8% using 1%, 3% and 5% Fe-TiO<sub>2</sub> under Visible light and 73.3%, 67.2% and 62.8% using 1%, 3% and 5% Fe-TiO<sub>2</sub> under UV light after irradiation for 80 Minutes respectively. It was noted from the results that the percentage degradation increases with increase in time of irradiation in respect to both UV/Fe-TiO<sub>2</sub> and Visible/Fe-TiO<sub>2</sub>. As time of irradiation increases more and more light energy falls on the catalyst surfaces which cause the generation of higher amount of photo excited species these are cause to increase the reactive oxygen species which are responsible to the generation of the adsorbed species.

#### 3.4.2. Effect of Metal Concentration in the Photo-degradation of Chlorazole Black E dye

In this section the percentage degradation of chlorazole black E was evaluated against various concentration of the modified catalyst which includes 1% FeTiO<sub>2</sub>, 3% FeTiO<sub>2</sub> and 5% FeTiO<sub>2</sub>. The studies involve 100ml  $1.0 \times 10^{-5}$  molar aqueous solution of chlorazole black E Dye with the catalyst amount of 0.2g from the result shown in Figure 9 and Figure 11. the percentage conversion was 67.2%, 74.8% and 62.8% using 1%, 3% and 5% Fe-TiO<sub>2</sub> under Visible light and 73.3%, 67.2% and 62.8% using 1%, 3% and 5% Fe-TiO<sub>2</sub> under UV light after irradiation for 80 Minutes respectively. However shows that the optimized catalyst are presented in order of activity 3% FeTiO<sub>2</sub> > 1% FeTiO<sub>2</sub> > 5% FeTiO<sub>2</sub> this indicated that an appropriate amount of dopant could suppress the recombination of photo-induce electron-hole pairs whereas the excess amount of dopant might cover the surface active site of the titania and decreased the photo quantum efficiency. The higher the activity of modified titania compared to pure titania is attributed to the effect of dopants which enhance the activity in visible light region by narrowing the band gap of the titania semiconductor.

#### 3.4.3. Effect of Light Source in the Photo-degradation of Chlorazole Black E dye

In this study 100ml  $1.0 \times 10^{-5}$  molar aqueous solution of chlorazole black E was used with catalyst amount of 0.2g of 1%, 3% and 5% Fe-TiO<sub>2</sub> and illumination of 80 minutes 280-400nm and 420-630nm was used for the source of UV and visible light respectively.

The percent photocatalytic degradation of chlorazole black E against the modified catalyst in both UV and Visible light are presented in Figures 9 and 11 the percentage conversion was 67.2%, 74.8% and 62.8% using 1%, 3% and 5% Fe-TiO<sub>2</sub> under Visible light and 73.3%, 67.2% and 62.8% using 1%, 3% and 5% Fe-TiO<sub>2</sub> under UV light after irradiation for 80 minutes respectively. However The result shows that both modified catalysts give higher activity in visible region and lower activity in UV light for the degradation of chlorazole black E. The higher activity of modified catalysts in visible light is attributed to the presence of dopant elements, which significantly reduces the crystalline size, reduces the band gap and controls the surface property through increase the surface area.

Fig-8. Rate of photocatalytic degradation of Chlorazole azo black E dye using 1% Fe-TiO<sub>2</sub>, 3% Fe-TiO<sub>2</sub> and 5% Fe-TiO<sub>2</sub> under UV light.

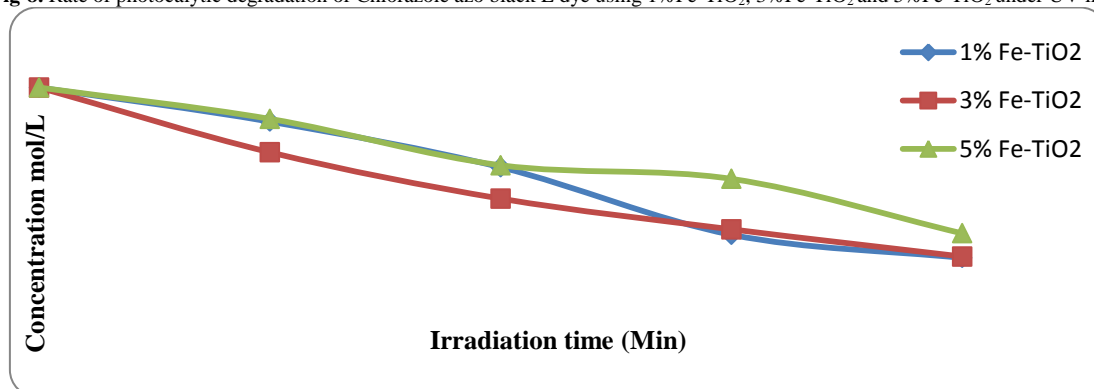
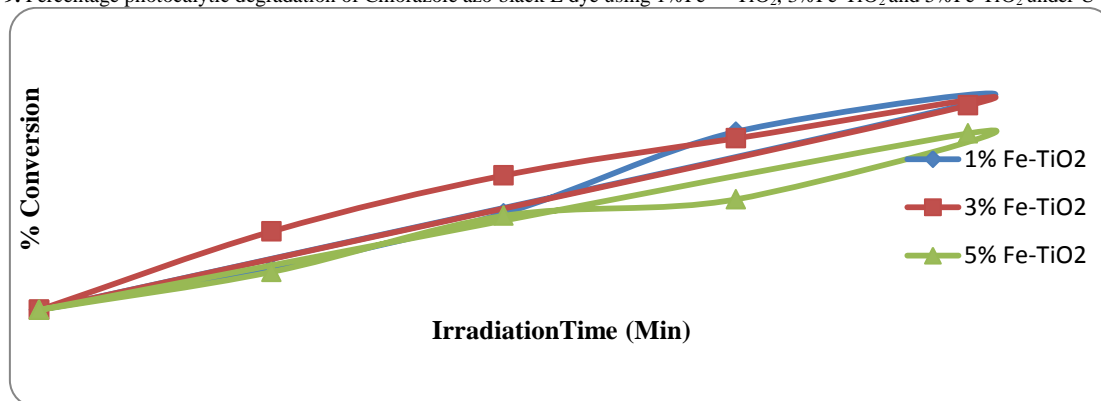
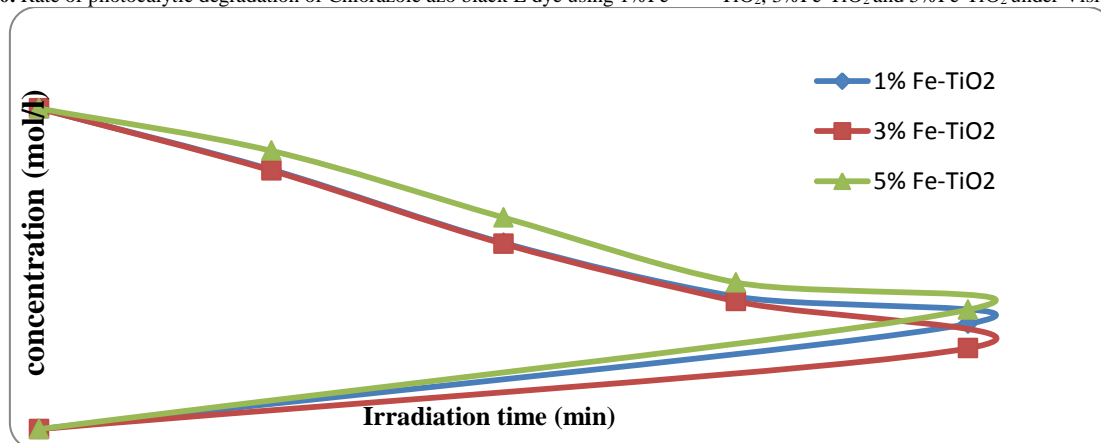
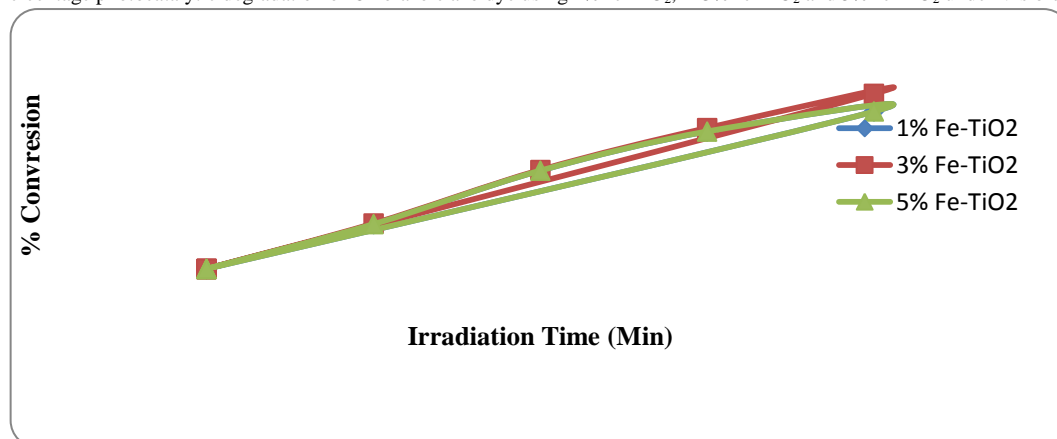


Fig-9. Percentage photocatalytic degradation of Chlorazole azo black E dye using 1%Fe- TiO<sub>2</sub>, 3%Fe-TiO<sub>2</sub> and 5%Fe-TiO<sub>2</sub> under UV light.Fig-10. Rate of photocatalytic degradation of Chlorazole azo black E dye using 1%Fe- TiO<sub>2</sub>, 3%Fe-TiO<sub>2</sub> and 5%Fe-TiO<sub>2</sub> under Visible light.Fig-11. Percentage photocatalytic degradation of Chlorazole azo dye using 1%Fe-TiO<sub>2</sub>, 3%Fe-TiO<sub>2</sub> and 5%Fe-TiO<sub>2</sub> under Visible-light

#### 4. Conclusion

The photocatalytic degradation of chlorazole black E in aqueous solution was studied using Fe-TiO<sub>2</sub> under UV and Visible light with different metal load concentration of 1% FeTiO<sub>2</sub>, 3% FeTiO<sub>2</sub>, and 5% FeTiO<sub>2</sub> catalyst. From the results shown in Figures 9 and 11 the percentage conversion was 67.2%, 74.8% and 62.8% using 1%, 3% and 5% Fe-TiO<sub>2</sub> under Visible light and 73.3%, 67.2% and 62.8% using 1%, 3% and 5% Fe-TiO<sub>2</sub> under UV light after irradiation for 80 Minutes respectively, effective photocatalytic degradation of chlorazole black E is available with the two light sources. Except that more decolourization was achieved using visible/Fe-TiO<sub>2</sub> with time. This is attributed to the present of dopant elements which significantly reduces the crystallite size, reduces the band gap and controls the surface property through increase in the surface area. However, 3%FeTiO<sub>2</sub> gives better results for both UV and Visible light, above this metal concentration there observed decrease in percentage photo degradation this may be due to the aggregation of catalyst particles at high concentration causing a decrease in the number of surface active sites.

## References

- [1] Laid, N., Bouanimba, N., Zouagh, R., and Sewili, T., 2014. "Study of the photocatalytic Degradations of Cationic Dyes in aqueous solution by different types of catalyst University of Constantine Algeria."
- [2] Khaataee, A. R. and Pons, M. N., 2009. "Photocatalytic degradation of three azo dyes using immobilized TiO<sub>2</sub> nanoparticles on glass plates activated by UV light irradiation: Influence of dye molecular structure." *Journal of Hazardous Materials*, vol. 168, pp. 451-457.
- [3] Syoufian, A. and Nakashima, K. J., 2008. "Degradation of methylene blue in aqueous dispersion of hollow titania photocatalyst: Study of reaction enhancement by various electron scavengers." *Coll. Inter. Sci.*, vol. 317, pp. 507-512.
- [4] Ge, X. L. M. and Fang, H. J., 2007. "Synthesis of titanium oxide layers on glass substrates with aqueous refluxed sols (rs) and photocatalytic activities." *Mater. Sci.*, vol. 42, pp. 4926-4934.
- [5] Forgacs, E. T. C. and Oros, G., 2004. "Removal of synthetic dyes from wastewaters." *A Review Environ. Int.*, vol. 30, pp. 953-971.
- [6] Brijesh, P., Dawid, S., Prakash, M., Themina, Q. T., and Thapak, R., 2011. "Mineralization of methylene violet dye using titanium dioxide in presence of visible light." *Int. J. Chem. Sci.*, vol. 9, pp. 1685-1697.
- [7] Chakraborty, R. and Roychowdhury, D., 2013. "Fish bone derived natural hydroxyapatite-supported copper acid catalyst: Taguchi optimisation of semi batch oleic acid esterification." *Chemical engineering journal*, vol. 215, pp. 491-499.
- [8] Di, P. A., Marci, G., Palmisano, L., Schiavello, M., Uosaki, K., Ikeda, S., and Ohtani, B., 2009. "Preparation of polycrystalline TiO<sub>2</sub> photocatalysts impregnated with various transition metal ions: Characterization and photocatalytic activity for the degradation of 4-nitrophenol." *J. Phys. Chem. B.*, vol. 106, pp. 637-645.
- [9] Kim, H. G., Hwang, D. W., and Lee, J. S., 2004. "An undoped, single-phase oxide photocatalyst working under visible light." *J. Am. Chem. Soc.*, vol. 126, pp. 8912-8913.
- [10] Zhou, Y., 2010. "A room-temperature reactive-template route to mesoporous ZnGa<sub>2</sub>O<sub>4</sub> with improved photocatalytic activity in reduction of CO<sub>2</sub>, Angew." *Chem. Int. ED.*, vol. 122, pp. 6544-6548.
- [11] Zhang, K. J., Xu, W., Li, X. J., Zheng, S. J., Xu, G., and Wang, J. H., 2006. "Photocatalytic oxidation activity of titanium dioxide film enhanced by Mn non-uniform doping." *Transactions of Nonferrous Metals Society of China*, vol. 16, pp. 1069-1075.
- [12] Navio, J. A., Colon, G., Macias, M., Real, C., and Litter, M. I., 1999. "Iron-doped titania semiconductor powders prepared by a sol-gel method—part I: synthesis and characterization." *Applied Catalysis*, vol. 177, pp. 111-120.
- [13] Sabry, M. and Abdel-Mottaleb, A., 2008. "Review article, increase of the photocatalytic activity of tio<sub>2</sub> by carbon and iron modifications, Hindawi." *International Journal of Photoenergy*, Available: <https://www.hindawi.com/journals/ijp/2008/721824/>
- [14] Zhu, J., Zheng, W. B., He, B., Zhang, J., and Anpo, M., 2004. "Characterization of Fe-TiO<sub>2</sub> photocatalysts synthesized by hydrothermal method and their photocatalytic reactivity for photodegradation of XRG dye diluted in water." *Journal of Molecular Catalysis A: Chemical*, vol. 216, pp. 35-43.
- [15] Zhu, J., Chen, F., Zhang, J., Chen, H., and Anpo, M., 2006. "Fe<sup>3+</sup>-TiO<sub>2</sub> photocatalysts prepared by combining sol-gel method with hydrothermal treatment and their characterization." *Journal of Photochemistry and Photobiology A: Chemistry*, vol. 180, pp. 196-204.
- [16] Adán, C., Bahamonde, A., Fernández-García, M., and Martínez-Arias, A., 2007. "Structure and activity of nanosized iron-doped anatase TiO<sub>2</sub> catalysts for phenol photocatalytic degradation." *Applied Catalysis B: Environmental*, vol. 72, pp. 11-17.
- [17] Siltür, F. and Say, M., 2009. "Effect of Fe<sup>3+</sup> ion doping to TiO<sub>2</sub> on the photocatalytic degradation of malachite green dye under UV and vis-irradiation." *Journal of Photochemistry and Photobiology A: Chemistry*, vol. 203, pp. 64-71.
- [18] Paola, S., Ohtani, B., and Palmisano, L., 2002. "Photocatalytic degradation of organic compounds in aqueous systems by transition metal doped polycrystalline TiO<sub>2</sub>." *Catalysis Today*, vol. 75, p. 87.
- [19] Di, P. A., Marci, G., Palmisano, L., Schiavello, M. K., Uosaki, K., Ikeda, S., and Ohtani, B., 2002. "Preparation of polycrystalline TiO<sub>2</sub> photocatalysts impregnated with various transition metal ions: Characterization and photocatalytic activity for the degradation of 4-Nitrophenol." *The Journal of Physical Chemistry B.*, vol. 106, pp. 637-645.
- [20] Ranjit, K. T. and Viswanathan, B., 1997. "Synthesis, characterization and photocatalytic properties of iron-doped TiO<sub>2</sub> catalysts." *Journal of Photochemistry and Photobiology A: Chemistry*, vol. 108, pp. 79-84.
- [21] Rhee, S. K., Lee, G. M., and Lee, S. T., 1996. *Appl. Microbiol. Biotechnol.*, vol. 44, pp. 816-822.
- [22] Ahmaruzaman, M., Ahmed, M. D. J. K., Begum, S., and Desalin, W. T., 2014. "Remediation of eriochrome black T-contaminated aqueous solutions utilizing H<sub>3</sub>PO<sub>4</sub>-modified berry leaves as a non-conventional adsorbent." *Desalination and Water Treatment*, vol. 56, pp. 1507-1519.
- [23] Lin, Q., Dhongui, W., and Jianlong, W., 2010. "Bioresour." *Technol.*, vol. 101, pp. 5229-5234.
- [24] Zhao, H., Xu, S., Zhong, J., and Bao, X., 2004. "Catal." *Today*, vol. 857, pp. 93-95.
- [25] Gupta, V. K., Jain, R., Mittal, A., Saleh, T. A., Nayak, A., Agarwal, S., and Sikarwar, S., 2012. *Mater. Sci. Eng., C.*, vol. 32, pp. 12-17.



- [26] Zhao, N. Q., Zhou, T. C., Shi, C. S., Li, J. J., and Guo, W. K., 2006. *Mater.Sci. Eng. B.*, vol. 127, pp. 207–211.
- [27] Suteu, D., Bilba, D., and Coseri, S., 2014. *J. Appl. Polym. Sci.*, vol. 131, pp. 39620–39631.
- [28] Bi, W., Hayes, R. B., Feng, P., Qi, Y., X., Y., and Zhen, J. J., 1992. *Am. J. Ind. Med.*, vol. 21, pp. 481-489.
- [29] Ahmed, M. D. J. K. and Ahmaruzzaman, M., 2015. *Water Sci. Technol.*, vol. 71, pp. 1361–1366.
- [30] Young, D. A., Mohammed, A. K., Blue, S. K., and Roberts, K. L., 2014. "Photocatalytic mineralization of chlorazol black e (direct black 38) over zeolite-supported titania-based catalysts." *J. Chem. Proc. Eng.*, vol. 1, p. 203.
- [31] Liu, A. R., Wang, S. M., Zhao, Y. R., and Zheng, Z., 2006. "Low temperature preparation of nanocrystalline TiO<sub>2</sub> photocatalyst with a very large specific surface area ISRN Materials Science 15." *Materials Chemistry and Physics*, vol. 99, pp. 131-134.